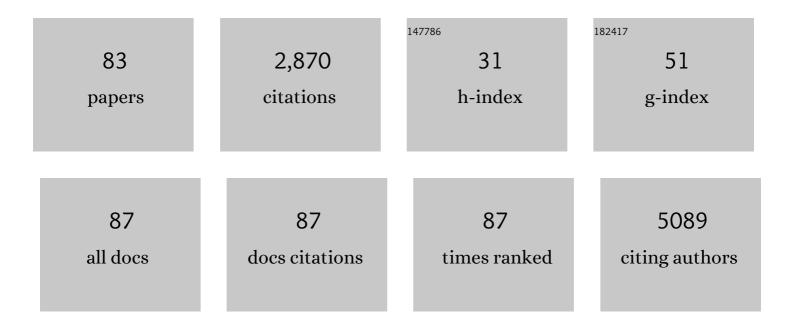
## Xingzhong Zhu

List of Publications by Year in descending order

Source: https://exaly.com/author-pdf/6035202/publications.pdf Version: 2024-02-01



XINCZHONC 7HU

#	Article	IF	CITATIONS
1	2D/2D 1Tâ€MoS <sub>2</sub> /Ti <sub>3</sub> C <sub>2</sub> MXene Heterostructure with Excellent Supercapacitor Performance. Advanced Functional Materials, 2020, 30, 0190302.	14.9	241
2	Gold Nanobipyramid-Directed Growth of Length-Variable Silver Nanorods with Multipolar Plasmon Resonances. ACS Nano, 2015, 9, 7523-7535.	14.6	135
3	Highly Ambient-Stable 1T-MoS <sub>2</sub> and 1T-WS <sub>2</sub> by Hydrothermal Synthesis under High Magnetic Fields. ACS Nano, 2019, 13, 1694-1702.	14.6	131
4	Au/Ag core–shell nanocuboids for high-efficiency organic solar cells with broadband plasmonic enhancement. Energy and Environmental Science, 2016, 9, 898-905.	30.8	127
5	Biosynthesis and Antibacterial Activity of Silver Nanoparticles Using Yeast Extract as Reducing and Capping Agents. Nanoscale Research Letters, 2020, 15, 14.	5.7	121
6	Gold Nanobipyramid‧upported Silver Nanostructures with Narrow Plasmon Linewidths and Improved Chemical Stability. Advanced Functional Materials, 2016, 26, 341-352.	14.9	119
7	Realization of Red Plasmon Shifts up to â^1⁄4900 nm by AgPd-Tipping Elongated Au Nanocrystals. Journal of the American Chemical Society, 2017, 139, 13837-13846.	13.7	96
8	Selective Pd Deposition on Au Nanobipyramids and Pd Siteâ€Đependent Plasmonic Photocatalytic Activity. Advanced Functional Materials, 2017, 27, 1700016.	14.9	94
9	Carbon-Encapsulated Metal/Metal Carbide/Metal Oxide Core–Shell Nanostructures Generated by Laser Ablation of Metals in Organic Solvents. ACS Applied Nano Materials, 2019, 2, 28-39.	5.0	86
10	Highly efficient and stable transparent electromagnetic interference shielding films based on silver nanowires. Nanoscale, 2020, 12, 14589-14597.	5.6	78
11	Two-dimensional CoNi nanoparticles@S,N-doped carbon composites derived from S,N-containing Co/Ni MOFs for high performance supercapacitors. Journal of Materials Chemistry A, 2017, 5, 9873-9881.	10.3	75
12	Unveiling highly ambient-stable multilayered 1T-MoS <sub>2</sub> towards all-solid-state flexible supercapacitors. Journal of Materials Chemistry A, 2019, 7, 19152-19160.	10.3	71
13	Design of Domain Structure and Realization of Ultralow Thermal Conductivity for Recordâ€High Thermoelectric Performance in Chalcopyrite. Advanced Materials, 2019, 31, e1905210.	21.0	61
14	Vapor-phase hydrothermal growth of single crystalline NiS2 nanostructure film on carbon fiber cloth for electrocatalytic oxidation of alcohols to ketones and simultaneous H2 evolution. Nano Research, 2018, 11, 1004-1017.	10.4	56
15	Ultrafine nickel–cobalt alloy nanoparticles incorporated into three-dimensional porous graphitic carbon as an electrode material for supercapacitors. Journal of Materials Chemistry A, 2016, 4, 17080-17086.	10.3	53
16	Gold nanobipyramid@cuprous oxide jujube-like nanostructures for plasmon-enhanced photocatalytic performance. Applied Catalysis B: Environmental, 2018, 234, 26-36.	20.2	52
17	Branched Silicon Nanotubes and Metal Nanowires via AAOâ€Templateâ€Assistant Approach. Advanced Functional Materials, 2010, 20, 3791-3796.	14.9	50
18	Titania oated Gold Nanoâ€Bipyramids for Blocking Autophagy Flux and Sensitizing Cancer Cells to Proteasome Inhibitorâ€Induced Death. Advanced Science, 2018, 5, 1700585.	11.2	50

#	Article	IF	CITATIONS
19	Enhanced thermoelectric performance of CuGaTe2 based composites incorporated with nanophase Cu2Se. Journal of Materials Chemistry A, 2014, 2, 2891.	10.3	49
20	Dielectric capacitors with three-dimensional nanoscale interdigital electrodes for energy storage. Science Advances, 2015, 1, e1500605.	10.3	49
21	Preferentially oriented large antimony trisulfide single-crystalline cuboids grown on polycrystalline titania film for solar cells. Communications Chemistry, 2019, 2, .	4.5	45
22	A Generic Synthetic Approach to Largeâ€Scale Pristineâ€Graphene/Metalâ€Nanoparticles Hybrids. Advanced Functional Materials, 2013, 23, 5771-5777.	14.9	42
23	Controllable Biosynthesis and Properties of Gold Nanoplates Using Yeast Extract. Nano-Micro Letters, 2017, 9, 5.	27.0	42
24	PET/Ag NW/PMMA transparent electromagnetic interference shielding films with high stability and flexibility. Nanoscale, 2021, 13, 8067-8076.	5.6	40
25	Facile chemical solution synthesis of p-type delafossite Ag-based transparent conducting AgCrO <sub>2</sub> films in an open condition. Journal of Materials Chemistry C, 2017, 5, 1885-1892.	5.5	39
26	Experimental and theoretical understanding on electrochemical activation and inactivation processes of Nb <sub>3</sub> O <sub>7</sub> (OH) for ambient electrosynthesis of NH <sub>3</sub> . Journal of Materials Chemistry A, 2019, 7, 16969-16978.	10.3	39
27	Self-curled coral-like $\hat{1}^3$ -Al 2 O 3 nanoplates for use as an adsorbent. Journal of Colloid and Interface Science, 2015, 453, 244-251.	9.4	38
28	Alloyed Au-Ag nanorods with desired plasmonic properties and stability in harsh environments. Photonics Research, 2019, 7, 558.	7.0	37
29	Gold nanobipyramid-embedded ultrathin metal nanoframes for <i>in situ</i> monitoring catalytic reactions. Chemical Science, 2020, 11, 3198-3207.	7.4	35
30	Gold Nanobipyramidâ€Enhanced Hydrogen Sensing with Plasmon Red Shifts Reaching â‰^140 nm at 2 vol% Hydrogen Concentration. Advanced Optical Materials, 2017, 5, 1700740.	7.3	34
31	Structure and thermal stability of gold nanoplates. Applied Physics Letters, 2006, 88, 071904.	3.3	33
32	Understanding the Solvent Molecules Induced Spontaneous Growth of Uncapped Tellurium Nanoparticles. Scientific Reports, 2016, 6, 32631.	3.3	31
33	Surfactant-free synthesis of Cu2O hollow spheres and their wavelength-dependent visible photocatalytic activities using LED lamps as cold light sources. Nanoscale Research Letters, 2014, 9, 624.	5.7	28
34	Oxygen Defects Induce Strongly Coupled Pt/Metal Oxides/rGO Nanocomposites for Methanol Oxidation Reaction. ACS Applied Energy Materials, 2019, 2, 5577-5583.	5.1	26
35	Fabrication of Stable and Flexible Nanocomposite Membranes Comprised of Cellulose Nanofibers and Graphene Oxide for Nanofluidic Ion Transport. ACS Applied Nano Materials, 2019, 2, 4193-4202.	5.0	25
36	Broadside Nanoantennas Made of Single Silver Nanorods. ACS Nano, 2018, 12, 1720-1731.	14.6	24

#	Article	IF	CITATIONS
37	Highly Uniform and Stable Transparent Electromagnetic Interference Shielding Film Based on Silver Nanowire–PEDOT:PSS Composite for High Power Microwave Shielding. Macromolecular Materials and Engineering, 2021, 306, 2000607.	3.6	24
38	Au tailored on g-C3N4/TiO2 heterostructure for enhanced photocatalytic performance. Journal of Alloys and Compounds, 2022, 894, 162338.	5.5	23
39	Molybdenum-Doped Porous Cobalt Phosphide Nanosheets for Efficient Alkaline Hydrogen Evolution. ACS Applied Energy Materials, 2019, 2, 6302-6310.	5.1	22
40	Synthesis of perfect silver nanocubes by a simple polyol process. Journal of Materials Research, 2007, 22, 1479-1485.	2.6	21
41	Construction of silica-encapsulated gold-silver core-shell nanorod: Atomic facets enrichment and plasmon enhanced catalytic activity with high stability and reusability. Materials and Design, 2019, 177, 107837.	7.0	21
42	Action Recognition Based on 3D Skeleton and RGB Frame Fusion. , 2019, , .		20
43	Self-powered ultraviolet photodetector based on an n-ZnO:Ga microwire/p-Si heterojunction with the performance enhanced by a pyro-phototronic effect. Optics Express, 2021, 29, 30244.	3.4	20
44	Growth and in situ transformation of TiO2 and HTiOF3 crystals on chitosan-polyvinyl alcohol co-polymer substrates under vapor phase hydrothermal conditions. Nano Research, 2016, 9, 745-754.	10.4	19
45	Synthesis of vertically oriented GaN nanowires on a LiAlO2 substrate via chemical vapor deposition. Nano Research, 2009, 2, 321-326.	10.4	17
46	Vertical La0.7Ca0.3MnO3 nanorods tailored by high magnetic field assisted pulsed laser deposition. Scientific Reports, 2016, 6, 19483.	3.3	17
47	Laserâ€Irradiationâ€Induced Melting and Reduction Reaction for the Formation of Ptâ€Based Bimetallic Alloy Particles in Liquids. ChemPhysChem, 2017, 18, 1133-1139.	2.1	17
48	Highly dispersed nickel anchored on a N-doped carbon molecular sieve derived from metal–organic frameworks for efficient hydrodeoxygenation in the aqueous phase. Chemical Communications, 2020, 56, 6696-6699.	4.1	17
49	Synthesis of carbon nanotubes on graphene quantum dot surface by catalyst free chemical vapor deposition. Carbon, 2014, 68, 399-405.	10.3	16
50	Selective Growth of Highâ€Density Anatase {101} Twin Boundaries on Highâ€Energy {001} Facets. Small Structures, 2020, 1, 2000025.	12.0	16
51	Enhanced thermoelectric performance of CuGaTe2 based composites incorporated with graphite nanosheets. Applied Physics Letters, 2016, 108, .	3.3	15
52	Molecular Sensitivities of Substrate-Supported Gold Nanocrystals. Journal of Physical Chemistry C, 2019, 123, 7336-7346.	3.1	14
53	Silver Nanowires Deposited on Cellulose Nanofibers/Graphene Oxide Hybrid Membranes as Sandwich-Structured Films for Optoelectronic and SERS Applications. ACS Applied Nano Materials, 2020, 3, 10844-10854.	5.0	14
54	Gold nanobipyramid-embedded silver–platinum hollow nanostructures for monitoring stepwise reduction and oxidation reactions. Nanoscale, 2020, 12, 23663-23672.	5.6	13

#	Article	IF	CITATIONS
55	A novel deposition mechanism of Au on Ag nanostructures involving galvanic replacement and reduction reactions. Chemical Communications, 2021, 57, 8332-8335.	4.1	12
56	The synthesis of silver nanowires with tunable diameters using halide ions for flexible transparent conductive films. CrystEngComm, 2020, 22, 8421-8429.	2.6	10
57	Crystal plane effect of ceria on supported copper catalyst for liquid-phase hydrogenation of unsaturated aldehyde. Journal of Colloid and Interface Science, 2021, 596, 34-43.	9.4	10
58	Hole structure and its formation in thin films of hydrolyzed poly(styrene maleic anhydride) alternating copolymers. Journal of Applied Polymer Science, 2000, 75, 267-274.	2.6	9
59	In situ synthesis of pristine-graphene/Ag nanocomposites as highly sensitive SERS substrates. RSC Advances, 2016, 6, 91579-91583.	3.6	9
60	Oneâ€Step and Surfactantâ€Free Fabrication of Goldâ€Nanoparticleâ€Decorated Bismuth Oxychloride Nanosheets Based on Laser Ablation in Solution and Their Enhanced Visibleâ€Light Plasmonic Photocatalysis. ChemPhysChem, 2017, 18, 1146-1154.	2.1	9
61	Dielectric function modelling and sensitivity forecast for Au–Ag alloy nanostructures. Physical Chemistry Chemical Physics, 2020, 22, 14932-14940.	2.8	8
62	Realization of red plasmon shifts by the selective etching of Ag nanorods. CrystEngComm, 2020, 22, 7870-7876.	2.6	8
63	Plasmonic O <sub>2</sub> dissociation and spillover expedite selective oxidation of primary C–H bonds. Chemical Science, 2021, 12, 15308-15317.	7.4	8
64	Surface-enhanced Raman scattering from plasmonic Ag-nanocube@Au-nanospheres core@satellites. Journal of Raman Spectroscopy, 2017, 48, 217-223.	2.5	7
65	(Cold triangular nanoplate core)@(silver shell) nanostructures as highly sensitive and selective plasmonic nanoprobes for hydrogen sulfide detection. Nanoscale, 2020, 12, 20250-20257.	5.6	7
66	Au nanobipyramids with Pt decoration enveloped in TiO <sub>2</sub> nanoboxes for photocatalytic reactions. Nanoscale Advances, 2021, 3, 4226-4234.	4.6	7
67	Synthesis of Pd nanorod arrays on Au nanoframes for excellent ethanol electrooxidation. Nanoscale, 2022, 14, 736-743.	5.6	7
68	Epitaxial Growth by Chemical Solution Deposition of (110) NdNiO <sub>3â^'Î&lt;</sub> Films with a Sharp Metalâ^'Insulator Transition Annealed under Ambient Oxygen. Crystal Growth and Design, 2010, 10, 4682-4685.	3.0	6
69	Photocatalytic Properties of SrTiO <sub>3</sub> Nanocubes Synthesized Through Molten Salt Modified Pechini Route. Journal of Nanoscience and Nanotechnology, 2016, 16, 12321-12325.	0.9	6
70	Surface modification effects on coercivity of the CoFe2O4 thin films with different thickness La0.7Sr0.3MnO3 layers. Journal of Applied Physics, 2017, 121, 245305.	2.5	6
71	Synthesis of porous Au–Ag alloy nanorods with tunable plasmonic properties and intrinsic hotspots for surface-enhanced Raman scattering. CrystEngComm, 2021, 23, 3467-3476.	2.6	6
72	Magneto-Revealing and Acceleration of Hidden Kirkendall Effect in Galvanic Replacement Reaction. Journal of Physical Chemistry Letters, 2021, 12, 5294-5300.	4.6	6

#	Article	IF	CITATIONS
73	Electrocatalytic glycerol oxidation enabled by surface plasmon polariton-induced hot carriers in Kretschmann configuration. Nanoscale, 2019, 11, 23234-23240.	5.6	5
74	Gold nanobipyramid enveloped in alloyed nanoshell for stable plasmonic sensors. Journal Physics D: Applied Physics, 2020, 53, 295303.	2.8	4
75	Revealing the truncated conical geometry of nanochannels in anodic aluminium oxide membranes. Nanoscale, 2022, 14, 5356-5368.	5.6	4
76	Synthesis of AuNi/NiO Nanocables by Porous AAO Template Assisted Galvanic Deposition and Subsequent Oxidation. European Journal of Inorganic Chemistry, 2010, 2010, 4309-4313.	2.0	3
77	Highly uniform hole spacing micro brushes based on aligned carbon nanotube arrays. Nanoscale Research Letters, 2013, 8, 501.	5.7	3
78	Sizeâ€Dependent Cytotoxicity of Thiolated Silver Nanoparticles Rapidly Probed by using Differential Pulse Voltammetry. ChemElectroChem, 2016, 3, 1197-1200.	3.4	3
79	Gold nanobipyramids doped with Au/Pd alloyed nanoclusters for high efficiency ethanol electrooxidation. Nanoscale Advances, 2022, 4, 1827-1834.	4.6	3
80	Mutual match for semi-supervised online evolutive learning. Applied Intelligence, 2023, 53, 3336-3350.	5.3	3
81	Structural transformation of Au seeds: the influence of temperature and surfactants. Journal of Nanophotonics, 2020, 14, 1.	1.0	2
82	A facile low-temperature growth of large-scale uniform two-end-open Ge nanotubes with hierarchical branches. Journal of Materials Chemistry C, 2013, 1, 5471.	5.5	1
83	Growth kinetics controlled rational synthesis of germanium nanotowers in chemical vapor deposition. Science China Materials, 2015, 58, 877-883.	6.3	0